THE JOURNAL OF PHYSICAL CHEMISTRY C
A JOURNAL OF THE AMERICAN CHEMICAL SOCIETY

pubs.acs.org/JPCC

Article

Structure and Formation of Luminescent Centers in Light-Up Ag Cluster-Based DNA Probes

Zakhar V. Reveguk, Vladimir A. Pomogaev, Marina A. Kapitonova, Andrey A. Buglak, and Alexei I. Kononov*

Cite This: *J. Phys. Chem. C* 2021, 125, 3542–3552

Read Online

ACCESS | Metrics & More | Article Recommendations | Supporting Information

ABSTRACT: Fluorescent beacons based on silver (Ag) clusters for DNA/RNA detection represent a new type of turn-on probe that fluoresces upon hybridization to target nucleobase sequences. Physical−chemical mechanisms of their fluorescence activation still remain poorly understood. We studied in detail the fluorescence activation of dark Ag clusters induced by interactions of Ag−DNA complexes with different DNA sequences. In all cases, the final result depends neither on the location of the precursors (dark clusters) nor on their spectral properties. The reaction of fluorescence activation is a process similar to the growth of fluorescent silver clusters on dsDNA matrices. In both cases, reactants are dark clusters and two adjacent DNA strands. The latter form a double-stranded template for cluster nucleation. We found the optimized structure of a green fluorescent Ag_4^{+2} cluster assembled on a C3/C3 DNA dimer in two different ssDNA pairs using QM modeling. The calculated absorption spectra match nicely the experimental ones, which proves the optimized structures. We conclude that apparent fluorescence activation in the studied systems results from reassembling Ag clusters on the new dsDNA template formed upon hybridization with the target. The suggested mechanism of "fluorescence activation" offers a way to design new light-up DNA probes. Two DNA strands making up the dsDNA template providing a high yield of bright Ag clusters can be used as the halves with the "stick" tails hybridizing with the base sequence of the target DNA. In this way, we have designed a light-up Ag cluster probe for *β-actin* mRNA.

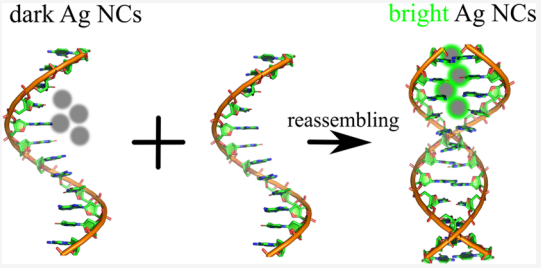

INTRODUCTION

Detection of specific nucleic acid sequences is of great importance in the area of medical diagnostics and therapeutics. DNA/RNA probes detect the presence of complementary nucleic acid sequences (target sequences) through hybridization. Such probes are typically labeled with isotopes, epitopes, or fluorophores, which allows the detection of their complexes with a target. In doing so, it is necessary to remove unbound probes, which can be difficult in many cases. In this respect, fluorescent "light-up" probes, which light up only in the presence of target DNAs, have a significant advantage due to a high ratio of fluorescence signals to the background. Molecular beacons based on the fluorescence resonance energy transfer (FRET) mechanism are often used as such light-up fluorescence probes.[1] High background in this case also reduces sensitivity toward DNA targets. A silver (Ag) cluster is a new alternative to conventional fluorescent probes.[2−4] Luminescent metal nanoclusters form a new class of luminophores extensively studied in the past decade.[5] They have a small size, high quantum yield, and high photostability.[6] Among them, DNA-based fluorescent silver clusters (Ag NCs) are rapidly gaining attention in the fields of biosensors and biological assays for their applications in detection of DNA,[7] single-nucleotide polymorphisms,[8] proteins,[9] and microRNA.[10] Fluorescent beacons based on Ag NCs for DNA/RNA detection are emerging as a new type of light-up probe that fluoresces upon hybridization with target nucleobase sequences.[2] Phenomenologically, the principle of their work is based on fluorescence enhancement effects when putting dark Ag NCs in close proximity to a guanine (G)-rich sequence. However, the physical−chemical mechanism of such enhancement still remains poorly understood. Since the first discovery of this effect in 2010,[7] various assumptions have been made. For example, it was suggested that guanines can serve as electron donors, reducing Ag clusters.[7] Another proposed explanation was that guanines can polarize the clusters, affecting their emission properties.[11] Later, Walczak et al. suggested that the enhancer sequence caused "reorganization" of Ag NCs.[12]

Guanine should not necessarily be an "enhancer". For example, poly-thymine (T) sequence caused green emission in the study of Yeh et al.[7] Petty et al. studied DNA sequences bearing a violet cluster that transformed into bright fluorescent

Received: November 4, 2020
Revised: January 22, 2021
Published: February 3, 2021

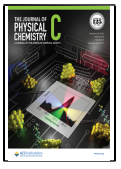

https://dx.doi.org/10.1021/acs.jpcc.0c09973
J. Phys. Chem. C 2021, 125, 3542−3552

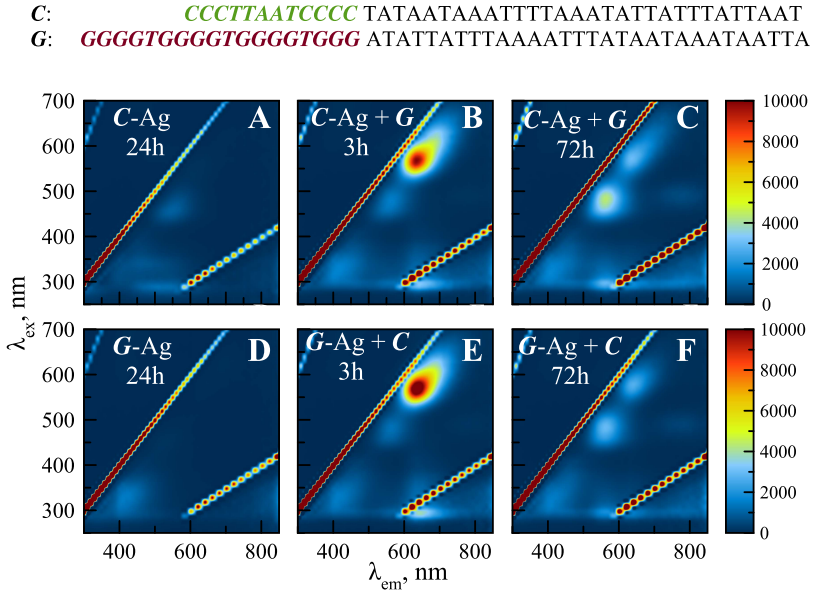

Figure 1. *C*- and *G*-strand DNA sequences (top). 2D fluorescence contour plots of Ag NCs on *C* and *G* strands in 24 h after the synthesis (A, D) and in 3 (B, E) and 72 h (C, F) after addition of the second strand.

ones from the blue-green to near-infrared regions upon hybridization with a shorter DNA target.[13−15] The authors suggested that the cluster moved between different binding sites.[15] One more example of a possible DNA probe was suggested in a recent study by Petty et al.[16] The authors split a DNA sequence yielding a fluorescent cluster into two halves, and after bringing them together, they synthesized the same cluster.

In this work, we studied in detail the fluorescence activation of dark Ag clusters induced by interactions of Ag−DNA complexes with different DNA sequences, including G-rich, adenine (A), and cytosine (C) sequences. We synthesized precursors (dark clusters/particles) both on the matrix and on the enhancer and also on the hybridized strands. We have found that in all cases the final result depends neither on the location of the precursors (dark clusters) nor on their spectral properties. The luminescent properties of the formed fluorescent complexes are determined by the matrix/enhancer interaction upon hybridization. In the case of cytosine-induced activation, we modeled the structure of the yellow-emitting fluorescent complex. We have shown that the chromophoric center of this complex consists of the Ag_4^{+2} cluster stabilized by a pair of C_3 tracts. We have concluded that apparent fluorescence activation in the studied systems results from reassembling of Ag clusters on the new dsDNA template formed upon hybridization with the target. Also, we have designed a light-up probe for detection of actin mRNA.

MATERIALS AND METHODS

Experiments. PAAG purified oligonucleotides were purchased from Evrogen (Moscow, Russia), and silver nitrate (99.99%) and sodium borohydride (>98%) were acquired from Sigma-Aldrich.

In a typical preparation, DNA (sodium phosphate pH 7.4, 50 mM) and $AgNO_3$ (aqueous solution) were mixed and incubated for 15 min at room temperature. Next, $NaBH_4$ aqueous solution was added and stirred vigorously for 2 min. Samples were kept at room temperature in the dark before measurements. All of the used DNA sequences are listed in Table S1. The final concentrations of DNA solutions are listed in Table S2.

Absorption spectra were acquired using a SPECORD 210 PLUS (Analytik Jena) spectrophotometer. Fluorescence spectra were measured using an F-6000 (Shimadzu) fluorimeter. The fluorescence quantum yield (QY) of Ag NCs on *S1*/*S2* strands was measured by a direct method using a Fluorolog-3 (HORIBA Jobin Yvon) spectrofluorometer and a Quanta-φ integrating sphere. Absorption and fluorescence measurements were carried out in a 4 mm path length quartz cuvette. The annealing process is carried out as follows: the samples were mixed with the appropriate buffer (sodium phosphate, pH 7.4, 50 mM) and then placed in a water bath heated to 95 °C, after which they were slowly cooled to room temperature.

QM Calculations. The double-stranded (ds) DNA sequences of 287 atoms 5′-(CCC)G-3′&3′-T(CCC)C-5′ (T-C_6-GC) and 318 atoms 5′-(CCC)AT-3′&3′-(CCC)TA-5′ (C_6-ATTA) were obtained using PyMOL v. 2.3.4, but excessive phosphates were deleted. Then, these dsDNA structures were used to produce complexes of Ag_4^{+2} clusters stabilized by ds cytosine trimers in these biopolymers (T-Ag_4@C_6-GC and Ag_4@C_6-ATTA, respectively). Distances between cytosines in duplexes of the original T-C_6-GC and C_6-ATTA were slightly extended to let Ag ions be spaced about 3 nm apart and more or less equally spread between these six nucleobases at a distance of 2−3.5 nm from the nearest nitrogen (N_3) and oxygen. Optimization was carried out in two stages. Stable Ag_4@DNA structures were obtained in the SMD continuum water model using the ONIOM[17,18] method implemented in Gaussian 16. The M062x functional with the hybrid basis sets def2-SVP[H]/def2-TZVP/def2-TZVPP[Ag] (M062X&def2-TZVP*) was used to optimize Ag_4@C_6 complexes, at a "high level", and the rest of the nucleobases and deoxyribose-phosphate backbone were calculated by PBE0&SVP, at a "low level". The M062x functional was approved earlier for silver−ligand complexes.[19−21] The final conventional optimization using the M062X&def2-SVP-[H,C,P]/def2-TZVP[N,O]/def2-TZVPP[Ag] approach was

https://dx.doi.org/10.1021/acs.jpcc.0c09973
J. Phys. Chem. C 2021, 125, 3542−3552

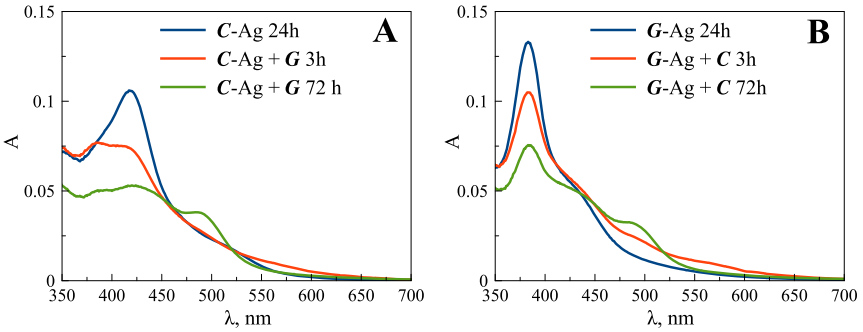

Figure 2. Absorption spectra of Ag NCs on *C* (A) and *G* strands (B) in 24 h after the synthesis and in 3 and 72 h after addition of the second strand.

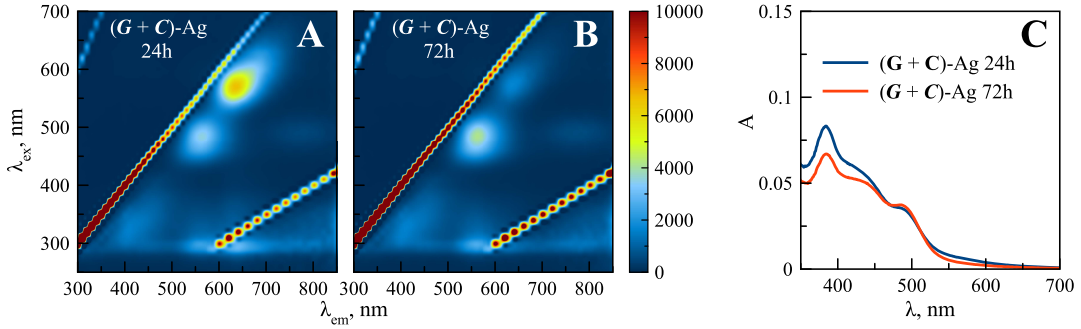

Figure 3. 2D fluorescence contour plots (A, B) and absorption spectra (C) of Ag NCs synthesized on prehybridized *C* and *G* strands.

applied to the chromophore $Ag_4@C_6$ complex, while the remaining molecular environment was frozen.

Complexes of silver clusters, stabilized with six cytosine moieties, were extracted from the optimal DNA structures to calculate excited states of absorption spectra. The bonds between the nucleobases and the deoxyribose-phosphate backbone were terminated and capped with hydrogen instead of the methyl group, typically used to mimic the electron-donating effect of the ribose group. Earlier, this approach was reported to be appropriate.[22] The electronic excitation (absorption) spectra of the complexes were calculated using the M062X&def2-TZVP* time-dependent density functional theory (TD-DFT) approach in Gaussian09, as well as the second-order algebraic-diagrammatic construction ADC(2) method[23] implemented in the Turbomole v.7.3 program package with the same basis sets, where 52 core MOs below −3.0 Hartree were frozen for calculations that significantly decreases the computational time without the loss of accuracy.

RESULTS

"Guanine/Cytosine-Proximity"-Induced Fluorescence Activation. First, we studied a well-known matrix/enhancer pair[7] consisting of AT-rich hybridizing tracts and also cytosine-rich and guanine-rich parts interacting upon hybridization (marked in Figure 1 as *C* and *G* strands, respectively). This is a classic case of the so-called "G-enhancement". In the first experiment, we synthesized Ag clusters on the *C* strand and then mixed the *C*-Ag complex with the *G* strand in 24 h. This experiment is illustrated in Figure 1A−C, representing the two-dimensional (2D) fluorescence contour color plot. A red cluster appeared after hybridization (Figure 1B). This result closely resembles the well-known results obtained in the literature.[7] Another Ag cluster, namely, a green cluster, was seen on the *C* strand even before the start of mixing (Figure 1A), and its luminescence increased after mixing. However, its excitation maximum at 460 nm shifted to 490 nm upon mixing (Figure S1), which implies some reorganization of the cluster. Then, the intensity of the red cluster decreased, while that of the green one increased (Figure 1C). Figure S2A,B shows the time evolution of the fluorescence spectra of both clusters. Thus, the red cluster appeared to be unstable. It insignificantly contributed to the absorption of the system (Figure 2), in contrast with the green one with an absorption maximum at 490 nm. This redistribution of red to green emission was attributed to oxidation of the red cluster.[12] However, it does not seem to be the case in the light of the fact that the degradation of the red cluster on prehybridized *C* and *G* strands (Figures 3 and S3) has nearly no effect on the intensity of the green cluster.

The changes observed in the absorption spectra (Figure 2) illustrate the reorganization processes with all species in solution after mixing. The absorption of the dark species at 420 nm on the *C* strand decreased, while the absorption of the green cluster increased. Under these experimental conditions, the red cluster insignificantly contributed to the absorption of the system as a weak long-wavelength tail that vanished in 72 h. Thus, both the green and red clusters were formed from the dark species when two strands were close together (probably with oxidation/reduction processes). The cluster transformation processes can be described by the following equation

$$C - \mathrm{Ag}(420, \mathrm{dark}) + G \rightarrow C - \mathrm{Ag} - G(560/620) + C - \mathrm{Ag} - G(490/560) \quad (1)$$

where *C*-Ag denotes the dark complex of silver with a *C*-rich sequence absorbing at 420 nm and *C*-Ag-*G* denotes the fluorescent complexes of the clusters with *C* and *G* strands.

https://dx.doi.org/10.1021/acs.jpcc.0c09973
J. Phys. Chem. C 2021, 125, 3542−3552

G6: 5' - *GGGGGG* TATAATAAATTTTAAATATTATTTATTAAT
A6: 3' - *AAAAAA* ATATTATTTAAAATTTATAATAAATAATTA

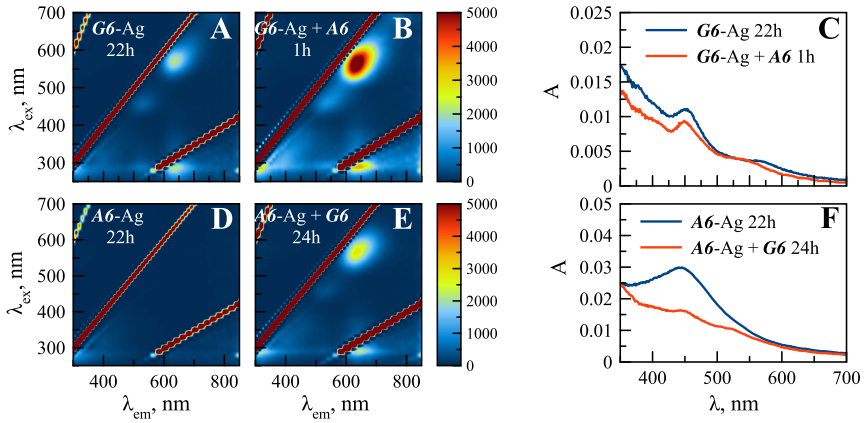

Figure 4. *G6* and *A6* DNA sequences (top). 2D fluorescence contour plots (left) and absorption spectra (right) of Ag NCs on *G6* and *A6* strands in 22 h after the synthesis and after addition of the second strand.

In the next experiment, which was performed for the first time, a DNA–Ag cluster was first synthesized on the *G* strand, and then, the *C* strand was brought together with the *G*-Ag complex. The as-synthesized *G*-Ag complex had no emission (Figure 1D). After mixing it with the *C* strand, both the green and red clusters appeared (Figure 1E,F). The 2D fluorescence contour plots appeared to be practically the same as it was in the first experiment when the *G* strand was added to the *C*-Ag complex (Figure 1). The time evolution of the fluorescence spectra is shown in Figure S2C,D. The process can be expressed by the following equation, similar to eq 1

$$G - \mathrm{Ag}(380, \mathrm{dark}) + C \rightarrow C - \mathrm{Ag} - G(500/560) + C - \mathrm{Ag} - G(560/620) \quad (2)$$

where analogously to (1) *G-Ag* denotes a dark complex of silver species with the *G*-rich sequence absorbing at 380 nm, and *C*-Ag-*G* denotes the fluorescent complexes of the clusters with *C* and *G* strands. The corresponding "gain coefficients", calculated as the ratio of the fluorescence intensities at the band maxima after and before mixing, are shown in Table S3. It appeared that the apparent gain of the emission was even greater in the case when the *C* strand served as an "enhancer" than in the case of "*G*-enhancer". The most remarkable thing, however, is that the final product appeared to be the same in both cases, although the precursors were different in the two cases. In the first case, the *C*-Ag precursor has a broad 420 nm absorption maximum (Figure 2A), while in the second case, the *G*–Ag species have a sharp maximum at 380 nm (Figure 2B). The different absorption spectra suggest different structures of the dark species. However, these different dark species were able to form the same fluorescent product. The absorption spectra collected in 72 h for two cases (Figure 2) are nearly identical in the visible range above 430 nm, where the main excitation peaks of the clusters are located. A significant difference in the range below 450 nm is evidently connected with the difference in the initial dark species on strands *C* and *G*. Not all of them turn into the luminescent product.

The luminescent product was formed as a result of interaction between the dark Ag cluster/particle and two single-stranded (ss) DNA fragments, *C* and *G*. Moreover, the same result was achieved when *C* and *G* strands were hybridized before the synthesis of Ag NCs (Figures 3 and S3). The fluorescent clusters were formed when two strands were brought together, meaning that the new clusters grew on the silver-mediated dsDNA template. It can be said that the dsDNA structure stabilizes the cluster.

Earlier it was shown that the interaction of the dark cluster on the *C* strand with the A_{12}-containing strand gave no emission, while interaction with C_{12} and T_{12} strands activated red and green fluorescence, respectively.[7] Relatively long 12-mer threads, interacting with silver, can fold into hairpin structures, which complicates interpretation. We explored the possible formation of the fluorescence clusters from the proximity of different short single-stranded (ss) DNA threads of six or three nucleotides in length.

"Adenine/Guanine-Proximity"-Induced Fluorescence Activation. Figure 4 shows the fluorescence activation for the *G6*/*A6* pair. The fluorescence of a weak red-emitting cluster on the G_6-bearing sequence (Figure 4A) was significantly increased (Figure 4B), and the absorption maximum was slightly shifted from 580 to 560 nm after mixing it with the A_6-bearing sequence and hybridization of the tails of these two strands (Figure 4C). We obtained the melting curves for both *G6*/*A6* and *G6*-Ag/*A6* mixtures (Figure S4), which proves the hybridization of AT tails in the absence as well as in the presence of Ag clusters. The bare AT strand was also added to the cluster on the *A6* strand (Figure S5a) and the bare TA strand to the cluster on the *G6* strand (Figure S5b). No effect was observed, which proves the role of the G_6 and A_6 tracts in the fluorescence enhancement. No fluorescence was also observed in the case when $AgNO_3$ and $NaBH_4$ were added to the hybridized *AT* tails without G_6 and A_6 tracts (Figure S6).

The same fluorescent cluster appeared when a dark cluster was first synthesized on the *A6* strand (Figure 4D) and when the *G6* strand was added (Figure 4E,F).

The observed chemical processes can be described as follows

$$G6 - \mathrm{Ag}(570/640, \mathrm{dim}) + A6 \rightarrow G6 - \mathrm{Ag} - A6(550/640, \mathrm{bright}) \quad (3)$$

https://dx.doi.org/10.1021/acs.jpcc.0c09973
J. Phys. Chem. C 2021, 125, 3542–3552

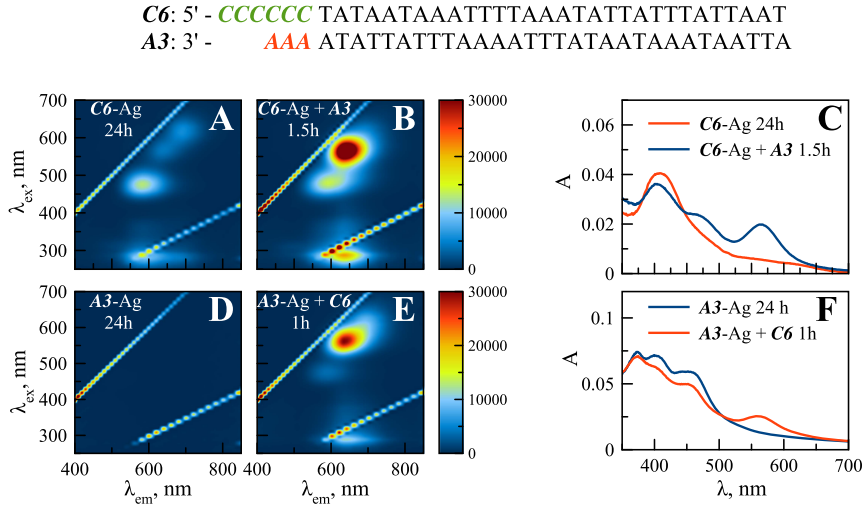

Figure 5. *C6* and *A3* DNA sequences (top). 2D fluorescence contour plots (left) and absorption spectra (right) of Ag NCs on *C6* and *A3* strands in 24 h after the synthesis and after addition of the second strand.

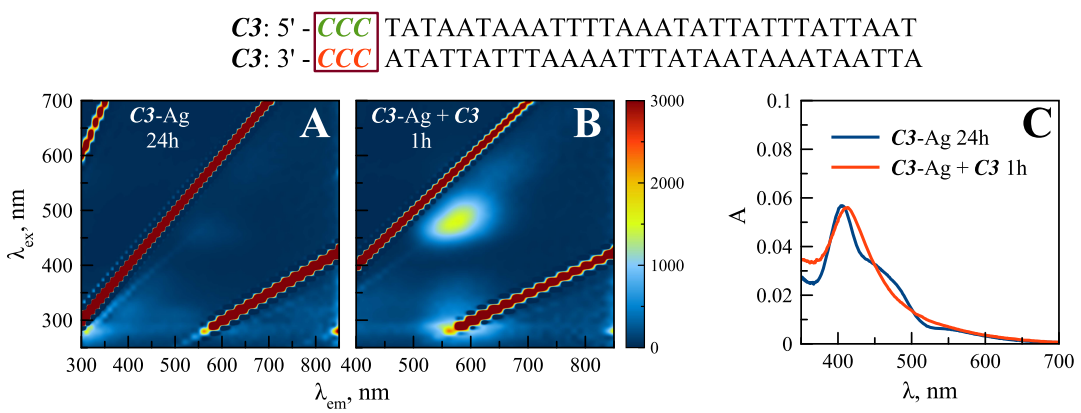

Figure 6. C_3-bearing strands of DNA sequences (top). 2D fluorescence contour plots (left) and absorption spectra (right) of Ag NCs on a single C_3-bearing strand in 24 h after the synthesis and after the second *C3* strand addition.

$$A6 - \mathrm{Ag}(440, \mathrm{dark}) + G6 \rightarrow A6 - \mathrm{Ag} - G6(550/640, \mathrm{bright}) \quad (4)$$

Like in the previous case of the *G/C* pair, the final result of processes (eqs 3 and 4) is the same and does not depend on which strand the precursor of the bright cluster was synthesized.

"Adenine/Cytosine-Proximity"-Induced Fluorescence Activation. In this experiment, a dominating dark species absorbing at 400 nm along with a small amount of a 580 nm emission cluster was synthesized on the C_6-bearing sequence (Figure 5A). In contrast to the above *G6/A6* case, addition of the *A6* strand in this case showed no fluorescence enhancement. However, after mixing the *C6* strand with the A_3-bearing sequence and hybridization of the tails of these two strands, a strongly emissive cluster appears at 640 nm (Figure 5B) with a pronounced absorption band at 550 nm (Figure 5C). The observed chemical process can be described by the following equation:

$$C6 - \mathrm{Ag}(400, \mathrm{dark}) + A3 \rightarrow C6 - \mathrm{Ag} - A3(560/640, \mathrm{bright}) \quad (5)$$

When in this pair we synthesized a dark cluster on the *A3* strand (Figure 5D) and then added the *C6* strand, we obtained the same 640 nm emitting cluster (Figure 5E,F). In this case, the *C6* strand serves as a "*C*-enhancer":

$$A3 - \mathrm{Ag}(400, \mathrm{dark}) + C6 \rightarrow A3 - Ag - C6(560/640, \mathrm{bright}) \quad (6)$$

"Cytosine/Cytosine-Proximity"-Induced Fluorescence Activation. The cytosine trimer in the ss C_3-bearing strand (*C3*) was not able to develop fluorescent clusters (Figure 6A). However, after the addition of the second C trimer, a green fluorescent cluster appeared (Figure 6B)

$$C3 - \mathrm{Ag}(410, \mathrm{dark}) + C3 \rightarrow C3 - \mathrm{Ag} - C3(490/560, \mathrm{bright}) \quad (7)$$

Also, a pronounced shoulder at about 500 nm appeared in the absorption spectrum (Figure 6C).

Sensor for Detection of mRNA Based on the Effect of "Cytosine−Cytosine Proximity". Next, we designed a fluorescent light-up probe for detection of *β-actin* messenger RNA (mRNA). This sensor consisted of two C-rich DNA sequences with the "stick" tails (*S1*, *S2* strands) hybridizing with two halves of the segment of the *β-actin* mRNA (*base*)

https://dx.doi.org/10.1021/acs.jpcc.0c09973
J. Phys. Chem. C 2021, 125, 3542−3552

(Figure 7A and Table S1). The sequences of the C-rich DNA parts were inspired by the study by Petty et al.,[16] where the

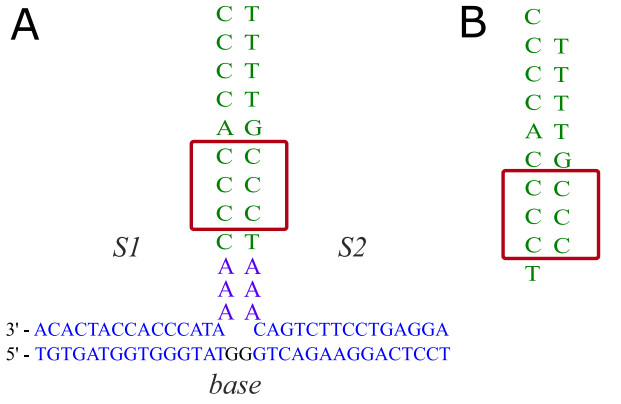

Figure 7. (A) Two C-rich DNA sequences with the "stick" tails (*S1*, *S2* strands) hybridizing with two halves of the segment of the *β-actin* mRNA (*base*). (B) Schematic possible structure of the C_4AC_4T/C_3GT_4 assembly of two DNA fragments developing a green-emitting Ag cluster obtained in ref 16.

authors split a DNA sequence yielding a green fluorescent cluster into two halves (Figure 7B), and after bringing them together, they synthesized the same bright cluster. We modified these two halves to get the highest chemical yield of the cluster, synthesized dark clusters on the halves, and studied how the spectral properties of the cluster were changed upon interaction with the other half. Two strands were appended to sequences that hybridized with the two halves of the segment of the *β-actin* of mRNA (Figure 7A and Table S1).

Figure 8 shows three series of experiments. First, Ag species were synthesized on the *S1* strand (left sequence in Figure 7A). The 2D fluorescence color map acquired in 22 h after synthesis is presented in Figure 8A. A fluorescent cluster with an excitation/emission maximum at 560/620 nm is seen on the map. Dark species with an absorption maximum at 400 nm are also seen in the absorption spectrum (Figure 7F). Then, *S2* (right sequence in Figure 7A) and *base* strands were added. We observed the time evolution of both the absorption and fluorescence emission spectra after the addition of *S2* and *base* strands. The absorption of the dark species at 400 nm rapidly decreased in the first 2 h, while a new absorption band appeared at 490 nm, and the absorption of the cluster at 560 nm decreased insignificantly (Figure S7). The appearance of the new absorption band was accompanied by the appearance of a new fluorescence band at 560 nm (Figures 8B and S8A). On a longer time scale, the red cluster at 620 nm degraded (Figures 8B and S8B). This process is not caused by interaction with the *S2* strand because the same degradation of the red cluster on the *S1* strand was observed in the absorption (Figure S9A) and emission (Figure S10B) spectra

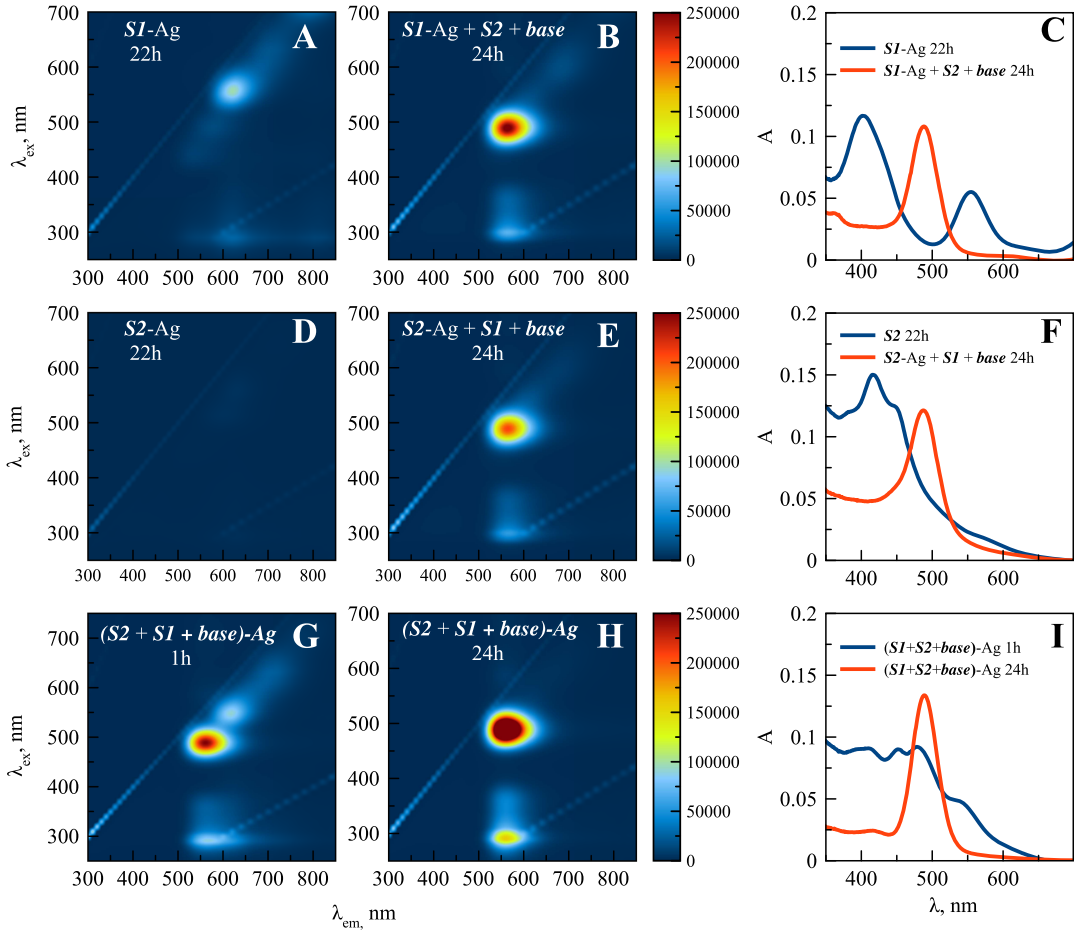

Figure 8. 2D fluorescence contour plots (left) and absorption spectra (right) of Ag NCs synthesized on single *S1* (A–C) and *S2* (D–F) strands before and after hybridization of *S1* and *S2* strands with the *base* strand and on prehybridized *S1*, *S2*, and *base* strands (G–I).

https://dx.doi.org/10.1021/acs.jpcc.0c09973
J. Phys. Chem. C 2021, 125, 3542–3552

on a longer time scale. Overall, the dark species with the absorption maximum at 400 nm degraded, and the emissive cluster with the absorption/emission maxima at 490 nm/560 nm appeared (Figure 8B,C). Overlapping absorption and excitation profiles suggest that the green cluster is a dominant product (Figure S11).

In the second experiment, we synthesized Ag precursor on the *S2* strand (Figure 8D,F) and then added *S1* and *base* strands (Figure 8E,F). In this case, the nonluminescent Ag precursor on the *S2* strand possessed an absorption spectrum, which was different from that of the dark species on the *S1* strand (Figure 8F). However, the reaction product was the same as that in the first experiment. The same green cluster with the absorption/emission maxima at 490/560 nm was formed (Figure 8E,F). The red cluster was also seen in the first hours after mixing of the strands and then was degraded (Figure S8D). Fluorescence and absorption kinetics of the clusters are presented in Figures S8−S10. A comparison of the dark precursors and the final products is presented in Figure S9C. In the third experiment, *S1* and *S2* strands were first hybridized with the halves of the *base* strand, and then, silver nitrate and borohydride were added to the solution. As a result, the same green emissive cluster was formed (Figure 8G−I). The corresponding "gain coefficients" and the QYs are shown in Table S4.

In this study, the synthesized Ag NCs were not purified by the HPLC. Therefore, there are many unlabeled DNA strands that can also be hybridized with the complementary strand. However, this does not seem to significantly affect the fluorescence activation. Addition of the same amount of unlabeled DNAs to solution after the synthesis of Ag NCs had a little effect on the gain coefficients (Table S4). It should also be noted that no "fluorescence activation" was observed in the absence of the *base* strand (Figure S12).

In all of the cases, although the precursors were different, the final results appeared to be nearly identical. The dominant product was the same green cluster as in the *C3*/*C3* case, absorbing at about 500 nm and emitting at 560 nm. In the first two experiments, the observed transformations can be expressed by the following equations

$$S1 - \mathrm{Ag}(400, \mathrm{dark}) + S2 \rightarrow S1 - \mathrm{Ag} - S2(490/560, \mathrm{bright}) \quad (8)$$

$$S2 - \mathrm{Ag}(420, \mathrm{dark}) + S1 \rightarrow S1 - \mathrm{Ag} - S2(490/560, \mathrm{bright}) \quad (9)$$

where, analogously to the previous equations, *S1*-Ag(400, dark) and *S2*-Ag(420, dark) denote the dark species on *S1* and *S2* strands, respectively, and *S2* → *S1*-Ag-*S2*(490/560, bright) denotes the fluorescent cluster stabilized by two strands.

Structure of the Fluorescent Complex. A common feature of all cases of fluorescence activation considered above is that the luminescence is activated when two DNA strands are forced together and a double-stranded structure stabilizing the emissive clusters is formed. This idea was further confirmed by theoretical calculations. We have modeled the structure of the chromophoric core of the cluster−DNA complexes for the "C-enhancement" case as an example of the common idea of dsDNA-induced fluorescence activation. In the beginning, we found the binding site of the chromophoric Ag core. The following observations were taken into account. First, the hybridizing AT-rich part of the DNA strands did not develop any fluorescent clusters, as shown above. Second, *C3*/*C3*, *S1*/*S2*, and C_4AC_4T/C_3GT_4 assemblies develop the same green-emitting 490/560 nm chromophore. The only same part of these assemblies is the C_3C_3 tract (highlighted in Figures 6 and 7 by a rectangle). This is evident in the *C3*/*C3* case (Figure 6). The same double-stranded region is also formed in the case of *β-actin* mRNA probe (Figure 7A) and in the case of the C_4AC_4T/C_3GT_4 assembly template,[16] the possible structure of which is shown in Figure 7B. The cluster lights up when two C_3 tracts are forced together. It can be deduced that in all of the cases the C_3C_3 ds tract is a binding site of the chromophoric core of the cluster. It should be emphasized here that the term "cluster" in the literature is usually applied to complexes of DNA with silver partially reduced by borohydride. The "size" of the cluster refers to the total amount of silver observed in the mass spectrum (MS) of the complex. It was found that the C_4AC_4T/C_3GT_4 template forms a green-emitting ten-silver complex with six Ag^+ ions and four Ag^0 atoms.[16] While in the case of bare metal clusters in the gas phase, the cluster size and the chromophore size are the same, for the Ag−DNA complexes, the size of the chromophoric core can be smaller than the apparent "size of the cluster" observed in MS, i.e., smaller than the overall number of silver atoms and cations bound to DNA. A significant part of Ag cations/atoms may not participate in the absorption and emission by the complex. The chromophoric core of the complex is what we mean here when we say "cluster", "cluster size", "cluster structure", etc. It is precisely the understanding of the structure of chromophoric centers in DNA−Ag complexes that is necessary, first, for understanding the mechanism of their fluorescence activation.

The cluster size, i.e., the number of silver atoms bound to the C_3C_3 template in this case and absorbing/emitting photons is the next question we address. Three-atomic clusters were earlier considered to interact with DNA through intercalation[24] or binding with C−Ag−C pairs.[25] However, their calculated absorption spectra in the complexes with DNA[25,26] do not match the absorption spectrum of the 560 nm green-emitting cluster. Therefore, we started with a four-atomic cluster. A positively charged cluster is expected based on the above-mentioned MS data[16] and on the theoretical calculations demonstrating that the charged clusters have much higher binding energies.[27] The fluorescence excitation spectra obtained for the fluorescent complexes place constraints on possible structures. Specifically, a strong excitation band lies in the visible range and another intensive band arises from DNA absorption at about 270 nm.[28] Thus, the lowest-energy S0−S1 transition is the most intense transition in the range from the visible region to the DNA absorption band at about 5 eV. For planar or three-dimensional Ag clusters, where each metal atom is bonded to at least two others, the absorption spectra of both free clusters[29−31] and their complexes with DNA[32,33] do not satisfy this condition. Typically, they exhibit low-intensity transitions in the visible range and strong absorption at 3.0−3.5 eV. The absorption spectra calculated for molecular dynamics (MD) simulated complexes of rod-shaped clusters with DNA[34] also do not reproduce the main feature observed in the experimental spectra, namely, a specific shape with a strong first transition and the absence of any strong transitions up to the UV absorption band of DNA. Instead, a threadlike shape of the Ag−DNA clusters was proposed to match the experimental fluorescence excitation spectra of the fluorescent

https://dx.doi.org/10.1021/acs.jpcc.0c09973
J. Phys. Chem. C 2021, 125, 3542−3552

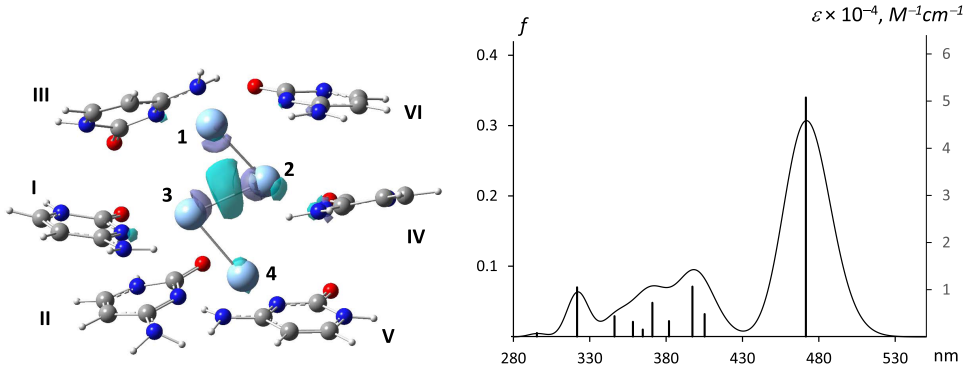

Figure 9. Left: Structure and electron density difference (EDD) isosurface map with an isovalue of 0.003 e^-/bohr^3 of the $Ag_4@C_6$ complex extracted from $Ag_4@C_6$-ATTA, where purple (blue) color indicates an increase (decrease) of the electron density for the lowest excitation. Right: Calculated absorption spectrum of the complex, oscillator strengths (f), and extinction coefficients (ε) for ten excited states (the spectrum is broadened by a Gaussian with a full width at half maximum (FWHM) of 0.2 eV, the same bandwidth as in the experimental spectrum).

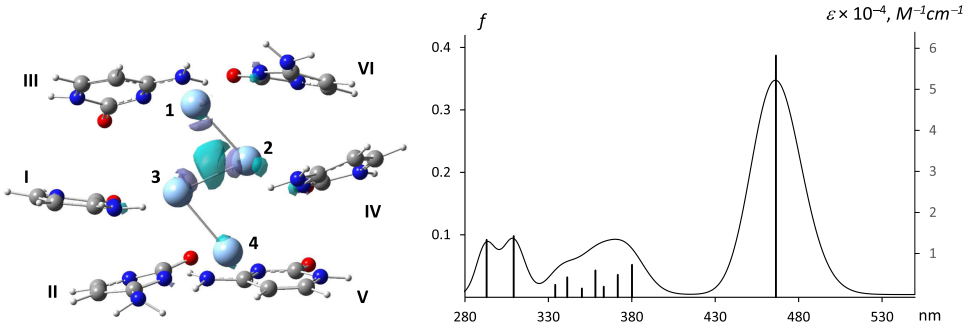

Figure 10. Left: Structure and EDD isosurface map with an isovalue of 0.003 e^-/bohr^3 of the $Ag_4@C_6$ complex extracted from T-$Ag_4@C_6$-GC, where purple (blue) color indicates an increase (decrease) of the electron density for the lowest excitation. Right: Calculated absorption spectrum of the complex, oscillator strengths (f), and extinction coefficients (ε) for ten excited states (the spectrum is broadened by a Gaussian with a FWHM of 0.2 eV, the same bandwidth as in the experimental spectrum).

complexes.[35] Several of these QM-optimized Ag−DNA complexes were presented in our previous works.[25,36] Their calculated spectra coincided very well with the experimental data. Therefore, we searched for a threadlike structure of the cluster stabilized by two C_3 tracts.

The initial structures of the ds templates stabilizing the cluster were constructed from two different short fragments of the duplexes shown in Figures 6 and 7, developing the same green cluster. One template was 5′-CCCAT-3′/3′-CCCTA-5′ assembly as a part of the structure shown in Figure 6. Another one was 5′-CCCG-3′/3′-TCCCC-5′ assembly, modeling the structure in Figure 7B. The optimization procedure is described in Materials and Methods in more detail.

Optimization of various initial Ag cluster configurations led to the most correct Ag cluster structures of a zigzag type, where each Ag atom is bonded to no more than two other Ag atoms, and the cluster has an extended threadlike shape close to that obtained earlier for the cluster stabilized by the C_4T_2 ds structure.[25]

ONIOM procedures did not yield the full equilibrium structures due to significant degrees of freedom. However, both $Ag_4@C_6$-ATTA and T-$Ag_4@C_6$-GC reached stable structures after several tens of iterations when structural fluctuations of chromophore $Ag_4@C_6$ complexes did not exceed 0.1 Å for noncovalent bonds of the silver cluster with the nearest atoms of the nucleobases and about 0.01 Å for Ag−Ag bonds through a hundred steps along the optimization trajectories (Tables S5 and S6). In the final step of optimization, the $Ag_4@C_6$ parts were optimized, while the rest of the atoms were frozen. Some structural parameters are shown in Tables S7 and S8. The resulting equilibrium structures of the $Ag_4@C_6$ chromophoric fragments extracted from the whole $Ag_4@C_6$-ATTA and T-$Ag_4@C_6$-GC final structures are presented in Figures 9 and 10, respectively.

Ten singlet excited states were calculated with TD-DFT, and five states were obtained using ADC(2) to establish the error of the TD-DFT method with regard to the more correct methods. The M06 functional was previously approved in comparison with the ADC(2) pure ab initio method.[19−21] The electronic excitation (absorption) spectra in the 516−300 nm band obtained in this work using M062X&def2-TZVP* agree well with the spectra calculated in the framework of ADC(2) &def2-TZVP* that is considered as a benchmark.[19−21] The spectra obtained using different approaches are presented in Table S9.

The calculated spectra fit nicely the experimental excitation and absorption spectra of the green cluster (Figures 6, 8, and S11), which proves the optimized structures. The maximum of the calculated spectrum appears to be very close to the experimental maximum. The more important thing, however, is that the spectra exhibit a specific shape with a strong first transition and the absence of any strong transitions up to the UV absorption band of DNA, which is typical for DNA-based Ag clusters.[28] Such a shape of the excitation spectra is explained by an extended (threadlike[35] or rodlike[37]) shape of the clusters. For comparison, a rhomb-like local minimum structure (Table S10) exhibits a weak S0−S1 transition, which does not agree with the experimental spectrum. In the

https://dx.doi.org/10.1021/acs.jpcc.0c09973
J. Phys. Chem. C 2021, 125, 3542−3552

zigzaglike structures (Figures 9 and 10), the strong S0−S1 transition is localized on the cluster with a small admixture of charge transfer to the bases. The higher electronic states have the pronounced charge-transfer character and low intensity (Table S9).

We also analyzed how the absorption spectrum changes with changes in the cluster size and charge. In doing so, we used models of free zigzaglike Ag clusters as well as the same clusters inserted into the C_6AT dsDNA manually with the Ag-base distances not less than 2.8 Å. The studied structures and their spectra in comparison with the spectrum of the optimized $Ag_4@C_6$ complex are presented in Table S11. Although the base−cluster interactions evidently cause red shifts in the absorption spectra of the complexes, a general tendency can be seen for both free clusters and complexes. As can be expected, an increase in the cluster size leads to a red shift of the spectrum (Table S11a). Thus, an increase in the cluster size from 4 to 6 atoms (while maintaining the number of confined electrons) leads to an increase in the energy of the S1 state by a factor of 1.3. Earlier, similar red shifts were reported for neutral and charged linear[35,38] and neutral zigzaglike[35] Ag clusters. An increase in the number of confined electrons in the Ag_4^0, Ag_5^{+1}, and Ag_6^{+2} zigzaglike clusters can lead to a significant decrease in the S1 oscillator strength.

The obtained cluster geometries for $Ag_4@C_6$-ATTA and T-$Ag_4@C_6$-GC complexes appear to be very similar to each other, although the sequences differ in bases adjacent to the C_3/C_3 dimer. Their spectra are also very similar to each other, which agrees nicely with the experimental data. Probably, the structure of the complex is mainly determined by the interaction of the silver core with the C_3/C_3 dimer rather than the base−base interactions between the neighboring bases. The calculated extinction coefficients ca. $5{\cdot}10^4$ $M^{-1}cm^{-1}$ (Figures 9 and 10) practically coincide with the experimental value obtained earlier for the cluster on the C_4AC_4T/C_3GT_4 assembly,[16] which also proves the proposed structure of the cluster. It is interesting to note that the obtained structure somewhat resembles the X-ray structure of a green Ag cluster found in ref 39, where a pentameric silver core interacts with six bases of an A_2C dimer. It should be noted that our calculations predict only the chromophoric core rather than the exact number of silver atoms/ions that can be observed, for example, in the experimental MS spectra or X-ray structures of the fluorescent Ag−DNA complexes. In addition to the metal core, which absorbs and emits photons, other silver ions/atoms can also stabilize the complex.

DISCUSSION

Our results lead to several main conclusions. First, strand dimers are necessary for emissive cluster growth. As our calculations show, for example, the C_3/C_3 dimer stabilizes the green-emitting cluster with a specific threadlike shape. The idea of an extended cluster shape was first proposed in the works of Gwinn et al.[37] and Kononov et al.[35] Obviously, such a structure requires two parallel DNA strands that would stabilize it. A cartoon structure of such a Ag−DNA complex with two DNA strands was suggested in ref 37. Based on the joint experimental and QM study, we presented some detailed structures of the Ag−DNA fluorescent clusters stabilized by two parallel DNA strands.[25,36] Two crystal structures of Ag−DNA complexes obtained to date[39,40] generally confirm the previously proposed models where an extended cluster is stabilized by two DNA strands. For example, in the X-ray structure described in ref 39, an A_2C dimer binds the Ag cluster core. In DNA solution, dsDNA templates can be realized due to self-dimer formation[41] or in the form of hairpins.[25] In the cases studied above, luminescence is activated when two DNA strands are forced together, which provides the necessary conditions for the formation of threadlike Ag clusters. Second, the fluorescent Ag clusters possess a unique threadlike structure that is totally different from that of the dark Ag precursors. Third, the same fluorescent Ag clusters are formed from different dark Ag precursors (dark clusters or particles) located on different DNA strands, as illustrated above, for example, by eqs 8 to 9. The order of the DNA additions can be altered. The final result depends on the base sequence in the new dimer template that is formed upon the close arrangement of two DNA strands. A new fluorescent complex is formed when an appropriate ds template, for example, C_3/C_3 dimer, appears. The two latter conclusions suggest disassembling the dark Ag species and then reassembling them into the threadlike structures in the presence of a strand dimer. Thus, "emission activation" is related to a dissolution of the dark species and reassembling of the clusters on the new double-stranded DNA template. Although it is known that DNA can etch Ag particles,[42] this does not seem to be the case here because the dark Ag species remained relatively stable in the presence of DNA, as can be seen, for example, in Figure S9. Most likely, these Ag species, observed in the 350−450 nm range, are relatively small Ag clusters of a planar or spherical shape, stabilized by DNA strands in solution. Moreover, similar dark Ag clusters are always visible at the initial stage of the traditional synthesis of luminescent clusters on DNA using silver nitrate and borohydride. At the first stage of synthesis, Ag^+ ions bind with the bases, and dsDNA templates form in hairpins[25] or in dimers via C−Ag^+−C or other silver-mediated pairing.[43] After the addition of borohydride, reduced silver atoms form dark clusters absorbing at about 400 nm, as can be seen, for example, in Figure 8I in an hour after mixing the reagents. Then, the dark clusters disappear, and the 490 nm absorption band of the green cluster becomes dominant (Figure 8I). This process is essentially no different from the process of "fluorescence activation", when dark clusters interact with two DNA strands and reassemble into fluorescent ones on ds templates. In this respect, the observed cases of fluorescence "enhancement" can be called "ds-template-induced nucleation of fluorescent Ag clusters".

It should be noted, however, that the interaction of both "matrix" and "enhancer" threads with the emissive cluster may not be necessary in some cases. The second hybridizing thread can lead to changes in the structural organization of the first DNA thread, which results in the growth of luminescent clusters on it. The example described in ref 15 is probably related to this case. Another example can be found in ref 7, where the red fluorescence activation observed in pair *C12/AT* was explained by a possible cluster -transfer process between the strands. In these cases, the emissive clusters are most likely stabilized by the hairpin ssDNA structures.

CONCLUSIONS

Summarizing the findings of this study, we conclude that all of the light-up Ag cluster-based sensors for a target DNA sequence work on the same mechanism. The reaction of fluorescence activation is a process similar to the growth of fluorescent silver clusters on dsDNA matrices. In both cases,

https://dx.doi.org/10.1021/acs.jpcc.0c09973
J. Phys. Chem. C 2021, 125, 3542−3552

reactants are dark clusters obtained by the reduction of silver ions with borohydride and two adjacent DNA strands. The latter form a double-stranded template for cluster nucleation. The nucleation efficiency of fluorescent Ag clusters depends on the ds template.

The fluorescence activation can be achieved using different ssDNA pairs. Examples of such activation are not only limited to guanine-rich sequences but also include cytosine-, adenine-, and even thymine-rich sequences. The final effect of the fluorescence light-up generally does not depend on which strand of the pair the Ag precursor (dark cluster) was synthesized first. The effect depends only on the chosen ssDNA pair. We have found the structure of a green fluorescent Ag_4^{+2} cluster assembled on the C_3/C_3 DNA dimer in two different ssDNA pairs using QM modeling. The calculated absorption spectra match nicely the experimental ones.

The suggested mechanism of "fluorescence activation" offers a way to design new light-up DNA probes. DNA strands making up dsDNA templates providing a high yield of bright Ag clusters should be identified first and then used as the halves with the "stick" tails hybridizing with the base sequence of the target DNA. In this way, we have designed a light-up Ag cluster probe for *β-actin* mRNA.

■ ASSOCIATED CONTENT

Supporting Information

The Supporting Information is available free of charge at https://pubs.acs.org/doi/10.1021/acs.jpcc.0c09973.

DNA sequences; synthesis conditions; and absorption, fluorescence emission, and fluorescence excitation spectra of Ag NCs; tables showing interatomic distances in the Ag NCs; DNA structures obtained after the ONIOM optimization; calculated energies and oscillator strengths of the lowest singlet excited states of the Ag NCs; and DNA complexes using different QM approaches (PDF)

■ AUTHOR INFORMATION

Corresponding Author

Alexei I. Kononov − *Department of Molecular Biophysics and Polymer Physics, Saint Petersburg State University, 199034 St. Petersburg, Russia;* orcid.org/0000-0001-5787-3599; Email: a.kononov@spbu.ru

Authors

Zakhar V. Reveguk − *Department of Molecular Biophysics and Polymer Physics, Saint Petersburg State University, 199034 St. Petersburg, Russia;* orcid.org/0000-0001-5475-3030

Vladimir A. Pomogaev − *Department of Physics, Tomsk State University, Tomsk 634050, Russia; Department of Chemistry and Green-Nano Materials Research Center, College of Natural Sciences, Kyungpook National University 1370 Sankyuk-dong, Buk-gu, Daegu 702-701, Republic of Korea;* orcid.org/0000-0003-4774-3998

Marina A. Kapitonova − *Department of Molecular Biophysics and Polymer Physics, Saint Petersburg State University, 199034 St. Petersburg, Russia*

Andrey A. Buglak − *Department of Molecular Biophysics and Polymer Physics, Saint Petersburg State University, 199034 St. Petersburg, Russia;* orcid.org/0000-0002-6405-6594

Complete contact information is available at: https://pubs.acs.org/10.1021/acs.jpcc.0c09973

Author Contributions

The manuscript was written through the contribution of all authors. All authors have given approval to the final version of the manuscript.

Notes

The authors declare no competing financial interest.

■ ACKNOWLEDGMENTS

This work was carried out using the equipment of the Centre for Optical and Laser Materials Research and the Centre for Diagnostics of Functional Materials for Medicine, Pharmacology, and Nanoelectronics at Saint Petersburg State University. The authors acknowledge RSF for research grant 16-13-10090. The theoretical part of this study was supported by RFBR grant 19-53-5100.

■ REFERENCES

(1) Juskowiak, B. Nucleic Acid-Based Fluorescent Probes and Their Analytical Potential. *Anal. Bioanal. Chem.* **2011**, *399*, 3157−3176.

(2) Obliosca, J. M.; Babin, M. C.; Liu, C.; Liu, Y.-L.; Chen, Y.-A.; Batson, R. A.; Ganguly, M.; Petty, J. T.; Yeh, H.-C. A Complementary Palette of NanoCluster Beacons. *ACS Nano* **2014**, *8*, 10150−10160.

(3) Liu, J. DNA-Stabilized, Fluorescent, Metal Nanoclusters for Biosensor Development. *TrAC, Trends Anal. Chem.* **2014**, *58*, 99−111.

(4) Chen, Y.; Phipps, M. L.; Werner, J. H.; Chakraborty, S.; Martinez, J. S. DNA Templated Metal Nanoclusters: From Emergent Properties to Unique Applications. *Acc. Chem. Res.* **2018**, *51*, 2756−2763.

(5) Chakraborty, I.; Pradeep, T. Atomically Precise Clusters of Noble Metals: Emerging Link between Atoms and Nanoparticles. *Chem. Rev.* **2017**, *117*, 8208−8271.

(6) Richards, C. I.; Choi, S.; Hsiang, J.-C.; Antoku, Y.; Vosch, T.; Bongiorno, A.; Tzeng, Y.-L.; Dickson, R. M. Oligonucleotide-Stabilized Ag Nanocluster Fluorophores. *J. Am. Chem. Soc.* **2008**, *130*, 5038−5039.

(7) Yeh, H.-C.; Sharma, J.; Han, J. J.; Martinez, J. S.; Werner, J. H. A DNA−Silver Nanocluster Probe That Fluoresces upon Hybridization. *Nano Lett.* **2010**, *10*, 3106−3110.

(8) Yeh, H.-C.; Sharma, J.; Shih, I.-M.; Vu, D. M.; Martinez, J. S.; Werner, J. H. A Fluorescence Light-Up Ag Nanocluster Probe That Discriminates Single-Nucleotide Variants by Emission Color. *J. Am. Chem. Soc.* **2012**, *134*, 11550−11558.

(9) Sharma, J.; Yeh, H.-C.; Yoo, H.; Werner, J. H.; Martinez, J. S. Silver Nanocluster Aptamers: In Situ Generation of Intrinsically Fluorescent Recognition Ligands for Protein Detection. *Chem. Commun.* **2011**, *47*, 2294−2296.

(10) Shah, P.; Rørvig-Lund, A.; Chaabane, S. B.; Thulstrup, P. W.; Kjaergaard, H. G.; Fron, E.; Hofkens, J.; Yang, S. W.; Vosch, T. Design Aspects of Bright Red Emissive Silver Nanoclusters/DNA Probes for MicroRNA Detection. *ACS Nano* **2012**, *6*, 8803−8814.

(11) Yau, S. H.; Abeyasinghe, N.; Orr, M.; Upton, L.; Varnavski, O.; Werner, J. H.; Yeh, H.-C.; Sharma, J.; Shreve, A. P.; Martinez, J. S.; Goodson, T., III Bright Two-Photon Emission and Ultra-Fast Relaxation Dynamics in a DNA-Templated Nanocluster Investigated by Ultra-Fast Spectroscopy. *Nanoscale* **2012**, *4*, 4247−4254.

(12) Walczak, S.; Morishita, K.; Ahmed, M.; Liu, J. Towards Understanding of Poly-Guanine Activated Fluorescent Silver Nanoclusters. *Nanotechnology* **2014**, *25*, No. 155501.

(13) Petty, J. T.; Giri, B.; Miller, I. C.; Nicholson, D. A.; Sergev, O. O.; Banks, T. M.; Story, S. P. Silver Clusters as Both Chromophoric Reporters and DNA Ligands. *Anal. Chem.* **2013**, *85*, 2183−2190.

(14) Petty, J. T.; Sergev, O. O.; Kantor, A. G.; Rankine, I. J.; Ganguly, M.; David, F. D.; Wheeler, S. K.; Wheeler, J. F. Ten-Atom

Silver Cluster Signaling and Tempering DNA Hybridization. *Anal. Chem.* **2015**, *87*, 5302−5309.
(15) Petty, J. T.; Sergev, O. O.; Nicholson, D. A.; Goodwin, P. M.; Giri, B.; McMullan, D. R. A Silver Cluster−DNA Equilibrium. *Anal. Chem.* **2013**, *85*, 9868−9876.
(16) He, C.; Goodwin, P. M.; Yunus, A. I.; Dickson, R. M.; Petty, J. T. A Split DNA Scaffold for a Green Fluorescent Silver Cluster. *J. Phys. Chem. C* **2019**, *123*, 17588−17597.
(17) Chung, L. W.; Sameera, W. M. C.; Ramozzi, R.; Page, A. J.; Hatanaka, M.; Petrova, G. P.; Harris, T. V.; Li, X.; Ke, Z.; Liu, F.; et al. The ONIOM Method and Its Applications. *Chem. Rev.* **2015**, *115*, 5678−5796.
(18) Dapprich, S.; Komaromi, I.; Byun, K. S.; Morokuma, K.; Frisch, M. J. A New ONIOM Implementation in Gaussian98. Part I. The Calculation of Energies, Gradients, Vibrational Frequencies and Electric FIeld Derivatives. *J. Mol. Struct.: THEOCHEM* **1999**, *461−462*, 1−21.
(19) Maksimov, D. A.; Pomogaev, V. A.; Kononov, A. I. Excitation Spectra of Ag 3 −DNA Bases Complexes: A Benchmark Study. *Chem. Phys. Lett.* **2017**, *673*, 11−18.
(20) Sych, T. S.; Reveguk, Z. V.; Pomogaev, V. A.; Buglak, A. A.; Reveguk, A. A.; Ramazanov, R. R.; Romanov, N. M.; Chikhirzhina, E. V.; Polyanichko, A. M.; Kononov, A. I. Fluorescent Silver Clusters on Protein Templates: Understanding Their Structure. *J. Phys. Chem. C* **2018**, *122*, 29549−29558.
(21) Buglak, A. A.; Pomogaev, V. A.; Kononov, A. I. Predicting Absorption Spectra of Silver-ligand Complexes. *Int. J. Quantum Chem.* **2019**, *119*, No. e25995.
(22) Reveguk, Z. V.; Khoroshilov, E. V.; Sharkov, A. V.; Pomogaev, V. A.; Buglak, A. A.; Tarnovsky, A. N.; Kononov, A. I. Exciton Absorption and Luminescence in I-Motif DNA. *Sci. Rep.* **2019**, *9*, No. 15988.
(23) Schirmer, J. Beyond the Random-Phase Approximation: A New Approximation Scheme for the Polarization Propagator. *Phys. Rev. A* **1982**, *26*, 2395−2416.
(24) Buceta, D.; Busto, N.; Barone, G.; Leal, J. M.; Domínguez, F.; Giovanetti, L. J.; Requejo, F. G.; García, B.; López-Quintela, M. A. Ag $_2$ and Ag $_3$ Clusters: Synthesis, Characterization, and Interaction with DNA. *Angew. Chem., Int. Ed.* **2015**, *54*, 7612−7616.
(25) Ramazanov, R. R.; Sych, T. S.; Reveguk, Z. V.; Maksimov, D. A.; Vdovichev, A. A.; Kononov, A. I. Ag−DNA Emitter: Metal Nanorod or Supramolecular Complex? *J. Phys. Chem. Lett.* **2016**, *7*, 3560−3566.
(26) Bonačić-Koutecký, V.; Perić, M.; Sanader, Ž. Why Do Silver Trimers Intercalated in DNA Exhibit Unique Nonlinear Properties That Are Promising for Applications? *J. Phys. Chem. Lett.* **2018**, *9*, 2584−2589.
(27) Buglak, A. A.; Kononov, A. I. Comparative Study of Gold and Silver Interactions with Amino Acids and Nucleobases. *RSC Adv.* **2020**, *10*, 34149−34160.
(28) O'Neill, P. R.; Gwinn, E. G.; Fygenson, D. K. UV Excitation of DNA Stabilized Ag Cluster Fluorescence via the DNA Bases. *J. Phys. Chem. C* **2011**, *115*, 24061−24066.
(29) Bonačić-Koutecky, V.; Veyret, V.; Mitrić, R. Ab Initio Study of the Absorption Spectra of Ag n (N=5−8) Clusters. *J. Chem. Phys.* **2001**, *115*, No. 10450.
(30) Harb, M.; Rabilloud, F.; Simon, D.; Rydlo, A.; Lecoultre, S.; Conus, F.; Rodrigues, V.; Félix, C. Optical Absorption of Small Silver Clusters: Agn, (N=4−22). *J. Chem. Phys.* **2008**, *129*, No. 194108.
(31) Baishya, K.; Idrobo, J. C.; Öğüt, S.; Yang, M.; Jackson, K.; Jellinek, J. Optical Absorption Spectra of Intermediate-Size Silver Clusters from First Principles. *Phys. Rev. B* **2008**, *78*, No. 075439.
(32) Soto-Verdugo, V.; Metiu, H.; Gwinn, E. The Properties of Small Ag Clusters Bound to DNA Bases. *J. Chem. Phys.* **2010**, *132*, No. 195102.
(33) Xi, C.; Boero, M.; Lopez-Acevedo, O. Atomic Structure and Origin of Chirality of DNA-Stabilized Silver Clusters. *Phys. Rev. Mater.* **2020**, *4*, No. 065601.
(34) Taccone, M. I.; Berdakin, M.; Pino, G. A.; Sánchez, C. Optical Properties and Charge Distribution in Rod-Shape DNA−Silver Cluster Emitters. *Phys. Chem. Chem. Phys.* **2018**, *20*, 22510−22516.
(35) Ramazanov, R. R.; Kononov, A. I. Excitation Spectra Argue for Threadlike Shape of DNA-Stabilized Silver Fluorescent Clusters. *J. Phys. Chem. C* **2013**, *117*, 18681−18687.
(36) Volkov, I. L.; Reveguk, Z. V.; Serdobintsev, P. Y.; Ramazanov, R. R.; Kononov, A. I. DNA as UV Light−Harvesting Antenna. *Nucleic Acids Res.* **2018**, *46*, 3543−3551.
(37) Schultz, D.; Gardner, K.; Oemrawsingh, S. S. R.; Markešević, N.; Olsson, K.; Debord, M.; Bouwmeester, D.; Gwinn, E. Evidence for Rod-Shaped DNA-Stabilized Silver Nanocluster Emitters. *Adv. Mater.* **2013**, *25*, 2797−2803.
(38) Guidez, E. B.; Aikens, C. M. Theoretical Analysis of the Optical Excitation Spectra of Silver and Gold Nanowires. *Nanoscale* **2012**, *4*, 4190−4198.
(39) Huard, D. J. E.; Demissie, A.; Kim, D.; Lewis, D.; Dickson, R. M.; Petty, J. T.; Lieberman, R. L. Atomic Structure of a Fluorescent Ag_8 Cluster Templated by a Multistranded DNA Scaffold. *J. Am. Chem. Soc.* **2019**, *141*, 11465−11470.
(40) Cerretani, C.; Kanazawa, H.; Vosch, T.; Kondo, J. Crystal Structure of a NIR-Emitting DNA-Stabilized Ag 16 Nanocluster. *Angew. Chem., Int. Ed.* **2019**, *58*, 17153−17157.
(41) Schultz, D.; Gwinn, E. G. Silver Atom and Strand Numbers in Fluorescent and Dark Ag:DNAs. *Chem. Commun.* **2012**, *48*, 5748−5750.
(42) Hu, S.; Wang, J.; Liu, J. Unified Etching and Protection of Faceted Silver Nanostructures by DNA Oligonucleotides. *J. Phys. Chem. C* **2019**, *123*, 12015−12022.
(43) Swasey, S. M.; Leal, L. E.; Lopez-Acevedo, O.; Pavlovich, J.; Gwinn, E. G. Silver (I) as DNA Glue: Ag+-Mediated Guanine Pairing Revealed by Removing Watson-Crick Constraints. *Sci. Rep.* **2015**, *5*, No. 10163.

https://dx.doi.org/10.1021/acs.jpcc.0c09973
J. Phys. Chem. C 2021, 125, 3542−3552